Cellulose
https://doi.org/10.1007/s10570-024-05869-x

ORIGINAL RESEARCH

Gamma radiation synthesis of hydroxyethyl cellulose/acrylic acid/CYANEX 471X hydrogel for silver ions capture from acidic nitrate medium

B. A. Masry · H. M. Gayed · J. A. Daoud

Received: 1 October 2023 / Accepted: 18 March 2024

Abstract The current novelty in this study is to recover silver ion with selective extractant such as cyanex 471X (triisobutylphosphine sulfide) through a clean and green method with high efficiency. Herein, a sustainable hydrogel (HEC/AAc/CX3) was fabricated from triisobutylphosphine sulfide, hydroxyethyl cellulose (HEC), and acrylic acid (AAc) using gamma irradiation polymerization and implanted for the sorption of silver Ag (I) ions from a nitrate acidic medium. Different techniques were employed for characterization of HEC/AAc/CX3 hydrogel such as FT-IR, SEM, XRD, and EDX, before and after the sorption process of Ag(I) ions. Gel content and swelling kinetics ratio of hydrogels at different irradiation doses (10, 20, 30, 40, and 50 kGy) were studied. The Fickian diffusion model results indicate that HEC/AAc/CX3 hydrogel is non-Fickian diffusion, which confirmed that the diffusion and relaxation rates are compatible and were selected for further sorption of Ag(I). The irradiated HEC/AAc/CX3 hydrogels, which contain 0.1 g of cyanex 471X, were employed for batch sorption of 100 mg/L Ag(I) from an acidic solution, and the suggested conditions were pH = 1, time = 60, and v/m = 0.05 L/g, which gives a sorption percentage of 75%. The values of thermodynamic parameters ΔH, ΔG, and ΔS were evaluated as—62.80 kJ/mol, 5 kJ/mol, and -227 J/mol, which indicate that the sorption system was exothermic and nonspontaneous in nature. The maximum adsorption capacity of irradiated HEC/AAc/CX3 for Ag(I) was found to be 12 mg. g^{-1} at 298 K. Furthermore, the maximum desorption percent of Ag ions from HEC/AAc/CX3 was found to be 70% and achieved with 0.5 M NH_4SCN after one desorption cycle. The prepared hydrogel proved its selectivity towards silver ions with facile desorption steps and reusability cycles.

Keywords HEC · Cyanex 471X · Hydrogel · Gamma irradiation · Silver · Acidic medium

B. A. Masry (✉) · J. A. Daoud
Hot Laboratories and Waste Management Center, Egyptian Atomic Energy Authority, Cairo 13759, Egypt
e-mail: betaam24@yahoo.com

H. M. Gayed (✉)
Radiation Research of Polymer Chemistry Department, National Centre for Radiation Research and Technology (NCRRT), Egyptian Atomic Energy Authority (EAEA), Cairo, Egypt
e-mail: hanygayed83@gmail.com; hany.gayed@eaea.org.eg

Introduction

One of the significant reserves of precious metals that could run out owing to overuse is silver (Hou et al. 2015; Li et al. 2018). Therefore, it is crucial to efficiently extract and recover silver ions in particular from wastewaters. Due to its high effectiveness, ease of use, and variety of adsorbent design, selective adsorption is one of the most popular

Published online: 05 April 2024

conventional water filtration methods (Min et al. 2019; Shao et al. 2019; Yu et al. 2019; Zou et al. 2019).

Sulfur atoms, which are electronegative donor atoms, have a great affinity for silver (I) ions (a soft Lewis acid) (Huang et al. 2019). Thus, the polymers with sulfur-containing functional groups as thiourea (Abd El-Ghaffar et al. 2009), thiolactone (Liu et al. 2018) cyanex 471X (Çelik et al. 2010) displayed remarkable selectivity in the adsorption of silver (I) ions.

Cyanex 471X was used for the recovery and extraction of platinum group metals such as silver (Fleitlikh et al. 2019), palladium (Ahmed et al. 2011; Kassem et al. 2017), platinum (Gupta et al. 2014) and gold (Duche et al. 2002) using different extraction techniques. Different polymers and hydrogels were used for the adsorption of silver from different media (Bundjaja et al. 2021; Song et al. 2012; Tran et al. 2019).

A hydrogel is a crosslinked network of hydrophilic polymers that can absorb and retain large amounts of water or aqueous solutions while maintaining their structural integrity (Behera and Mahanwar 2020; Gulrez et al. 2011; Saini 2017; Sun et al. 2021). With unique properties such as high-water content, softness, flexibility, and biocompatibility, hydrogels have found diverse applications in fields such as drug delivery, tissue engineering, metal recovery, sensors, and environmental remediation (Elella et al. 2021; Jacob et al. 2021; Maziad et al. 2016; Mohapatra et al. 2021). Although synthetic polymer-based products are commonly available (Madduma-Bandarage and Madihally 2021), there is extensive research on creating hydrogels from renewable materials such as polysaccharides, amino acids, and peptides, which are cost-effective and environmentally friendly (Kumar and Christopher 2017; Padil et al. 2018; Qi et al. 2021). These materials, including cellulose and its derivatives, are being studied for their potential applications, due to their biodegradability and other desirable properties (Foroughi et al. 2021; Kabir et al. 2018; Sannino et al. 2009). In particular, recent studies have focused on the water solubility and gel formation of cellulose derivatives, as cellulose is a widely available and inexpensive renewable resource (Oprea and Voicu 2020). Hydroxyethyl cellulose (HEC) is a biocompatible and biodegradable polymer that has shown great potential in various applications, including drug delivery, tissue engineering, and coatings (Janmohammadi et al. 2023; Zulkifli et al. 2017). HEC is water-soluble and can form hydrogels with unique properties, such as high swelling capacity, mechanical flexibility, and metal adsorption capability (Sabbagh et al. 2019).

Gamma radiation synthesis has emerged as a promising method for the modification of polymers, including HEC, due to its ability to induce controlled crosslinking and degradation, leading to the formation of hydrogels with tailored properties (Ashfaq et al. 2020; Gayeda et al. 2019; Raafat et al. 2012; Rimdusit et al. 2012). Gamma radiation can effectively crosslink HEC chains, resulting in hydrogels with improved stability and mechanical strength (Rimdusit et al. 2012). Additionally, gamma radiation can introduce functional groups onto the HEC backbone, enhancing its metal adsorption capacity (Kang et al. 2015). The recovery of metal ions from aqueous solutions has become a critical environmental concern due to the increasing contamination of water sources by heavy metals (Aly et al. 2021; 2022; Masry and Daoud 2021; Masry et al. 2023a; 2023b). Conventional methods for metal recovery, such as chemical precipitation and adsorption onto solid surfaces, often suffer from limitations such as low selectivity, complex operation, and high cost (Jin and Zhang 2020). Different materials and adsorbent were used for the capture and removal of precious metal ions such as silver ions (Allahyar and Özeroğlu 2022), platinum (Masry et al. 2018) from different aqueous media.

As a result, there is a growing interest in the development of innovative and sustainable materials for metal recovery. In this study, we aim to investigate the synthesis of HEC/AAc/CX3 hydrogels for silver recovery using gamma radiation. The effects of gamma radiation on the properties of HEC, gel fraction, swelling properties and metal adsorption capacity, will be systematically studied. The potential of HEC hydrogels synthesized via gamma radiation for metal recovery applications will be explored, highlighting their advantages and potential challenges. The findings of this study could provide valuable insights into the development of efficient and sustainable hydrogel-based materials for metal recovery, with potential implications in environmental and industrial applications. To the best of our knowledge, no previous studies have specifically investigated the

gamma radiation synthesis of HEC/AAc/CX3 hydrogels for silver recovery, making this research novel and significant in the field of polymer materials for environmental applications. The prepared hydrogel has many advantages, including low cost, easy operation, and no secondary pollution.

Expermental

Materials and reagents

Hydroxyethyl cellulose (HEC) and acrylic acid (AAc) were purchased from LOBA Chemie. All the reagents and chemicals used in this research are of analytical reagent grade (AR). CYANEX 471X (CX) which is a triisobutylphosphine sulfide (TIBPS) extractant, structure (1), is a solid soft Lewis base and readily interacts with metals that exhibit the characteristics of soft Lewis acids; it was kindly supplied by CYTEC (Canada) and used as received.

Irradiation processes

At the National Centre for Radiation Research and Technology, (NCRRT), Egyptian Atomic Energy Authority (EAEA), Nasr City, Cairo, Egypt, the HEC and AAc were exposed to radiation using Co-60—γ-cell -220 sources (manufactured by the Atomic Energy Authority) at various dose (10, 20, 30, 40, and 50) at approximately dose rate of 0.9 kGy/h.

Synthesis of HEC/AAc with CX hydrogels

Firstly, a hydroxyethyl cellulose solution (1%) was prepared by dissolving 1.0 g of HEC in 100 ml of distilled water and stirring for 2 h at 50 °C. Then 3 mL of acrylic acid was added to 7 mL of HEC solution and stirred for 1 h. Acrylic acid was employed in the creation of a hydrogel exhibiting satisfactory mechanical characteristics. This was achieved through the incorporation of cyanex, known for its unique metal absorption properties. The CX (Cyanex 471X) was added to the mixed solution and stirred well for 3 h with different concentrations of 0.01, 0.05, 0.1, and 0.2 (CX1 to CX4). Finally, the solutions were put into glass tubes that were sealed and subjected to varying amounts of gamma radiation. To eliminate the unreacted components after gamma radiation exposure, the samples are submerged in distilled water for 24 h. The samples are denoted (CX1-4) as shown in Table 1. Figure 1 show the preparation schematic diagram of prepared hydrogels.

Determination of gel fraction

Approximately 0.5 g of all irradiated samples were initially air-dried for approximately 24 h. Subsequently, they were dried in an oven at 60°C until a constant weight was achieved. The samples were then immersed in distilled water for 24 h to remove the unreacted part, followed by drying to a constant weight again. The extracted samples were then oven-dried until a constant weight was obtained. The gel content was determined gravimetrically using Eq. 1.

$$\text{Gelation } (\%) = \frac{w_g}{w_0} \times 100 \quad (1)$$

where W_g is the weight of dry gel after extraction in water and W_0 is the initial weight of dry gel (Krklješ et al. 2007).

Swelling kinetics of hydrogels

The dry hydrogels, which were prepared by irradiation, were allowed to swell in distilled water at room temperature. At regular intervals, the samples were weighed using an electronic balance after drying the surface with filter paper, and then returned to distilled water. Measurements were continued until the weight of all samples stabilized, indicating they had reached equilibrium. The swelling ratio (SR) of each hydrogel was calculated using Eq. 2 (Maziad et al. 2016; Süren et al. 2023).

$$SR = \frac{M_t - M_0}{M_0} \quad (2)$$

where M_t is the weight of swollen gel at time t and M_0 is the weight of dry gel at time 0. To determine the swelling kinetics of hydrogels, the data were fitted to Korsmeyer-Peppas Eq. 3 (Mingcheng et al. 2007).

The water absorption process in a three-dimensional hydrogel structure has been elucidated through the interplay of diffusion and macromolecular relaxation within the three-dimensional

Structure 1 Chemical structure of Cyanex 471X (TIBPS)

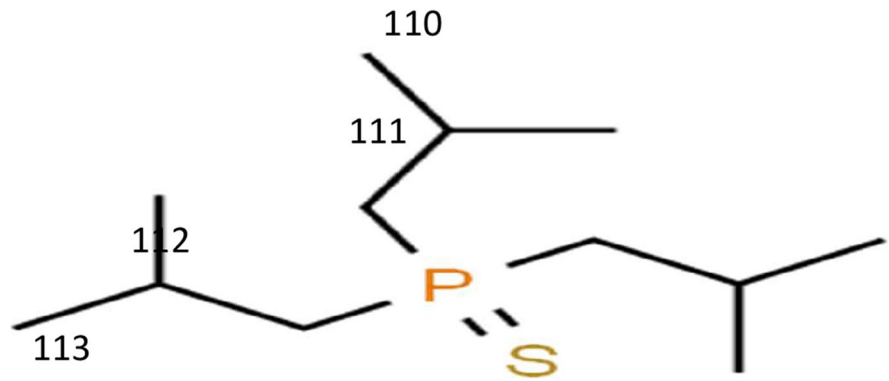

Table 1 Composition of prepared hydrogels

Hydrogels	HEC (1%)	AAc (mL)	CYANEX 471X (gm)
HEC/AAc	7 mL	3 mL	0
HEC/AAc/CX1	7 mL	3 mL	0.01
HEC/AAc/CX2	7 mL	3 mL	0.05
HEC/AAc/CX3	7 mL	3 mL	0.10
HEC/AAc/CX4	7 mL	3 mL	0.2

structure. This methodology is associated with Fickian diffusion processes, wherein the dimensionless exponent (n) serves as a key parameter defining the overall mechanism. The dimensionless exponents (i.e., n) were determined by analyzing the log–log slope of Mt/M∞ versus time, as outlined in Eq. (3), to characterize H_2O diffusion into different hydrogels.

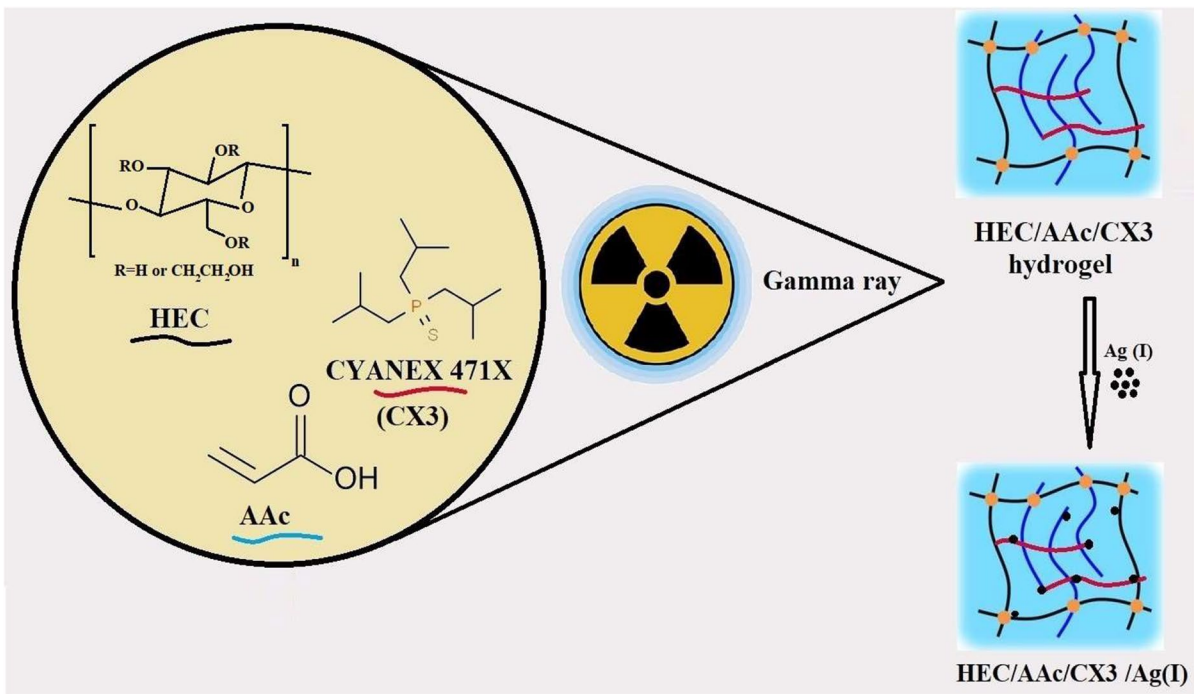

Fig. 1 Preparation schematic diagram of HEC/AAc/CX hydrogels

$$F(\%) = \frac{M_t}{M_\infty} = kt^n \quad (3)$$

where F is the fraction uptake of swelling, M_t is the weight of the sample at time 'T' and M_∞ is the weight of the sample at equilibrium, K is a constant, and n is the diffusional exponent, which ultimately determined the transport mechanism of hydrogel. To determine the type of diffusion of water into hydrogels, the simple and commonly used method, based on the power-law expression (Saraydın et al. 2018), was applied to equation no. 3 (Bajpai and Dubey 2004). To calculate the exponent n and constant K, the data was plotted on log–log plots according to Eq. 4, and the resulting curves were estimated using linear functions.

$$\log\left(\frac{M_t}{M\infty}\right) = \text{Logk} + \text{nlogt} \quad (4)$$

Characterization techniques

Fourier transforms infrared spectroscopy (a Nicolet Avatar 320 FT-IR Spectrophotometer, Cambridge, UK) with wave numbers ranging from 4000 cm^{-1} to 400 cm^{-1} was used. The surface of the samples was examined by SEM (Jeol, JSM, Japan) at a voltage of 30 kV. XRD patterns were recorded by the X-ray diffractometer (model: Shimadzu XRD-6000). XRD patterns are obtained in the range of 2θ from 4° to 90° at room temperature. Cu Kα is used as a radiation source of wavelength λ = 0.15408 nm and other operating conditions are scan rate 8°/min, and the operation voltage and current were 40 kV and 30 mA, respectively. The Ag-hydrogel was produced through chemical reduction using NaBH4. Following the absorption experiment, the prepared hydrogel underwent wiping with a wet filter paper to eliminate residual Ag ions from its surface. Subsequently, it was immersed in a cold aqueous solution of $NaBH_4$ (20 mM) for 12 h. Afterward, the hydrogel underwent a 2-day rinsing process in deionized water.

Adsorptive studies

To estimate the uptake efficiency of the prepared gamma irradiated (HEC/AAc/CX) hydrogel, a known weight of 0.1 g of each adsorbent was shaken with 5 mL of 100 mg/L Ag(I) in an aqueous acidic nitrate solution of pH = 1 for 60 min at 25 ± 1°C in a thermostated water shaker. After the filtration of the two phases, the concentration of Ag(I) ions was determined using atomic absorption spectrometer (AAS-Thermo Fisher-USA). All experiments were three-checked for accuracy to verify that the findings were applicable. Equation 5 (Noweir et al. 2021): provides the sorption percentage of Ag(I) ions in each experiment.

$$S\% = \left(\frac{C_i - C_e}{C_i}\right) \times 100 \quad (5)$$

where C_i and C_e are the initial and equilibrium concentrations (mg/g) of Ag(I) in the aqueous solution. The sorption capacity q_e at equilibrium is given by the following Eq. 6 (Aly et al. 2022):

$$q_e = (C_i - C_e) \times \frac{V}{m} \quad (6)$$

where V is the volume of the used aqueous antinomy solution (L) and m is the weight of (HEC/AAc/CX) adsorbent (g).

Results and discussion

FTIR measurements

The FTIR spectrum of hydroxyethyl cellulose is shown in Fig. 2a; the absorption band at 3411 cm^{-1} is ascribed to O–H stretching vibration, and the bands at 2974 cm^{-1} attributed to C–H aliphatic stretching vibrations (Kajjari et al. 2011). The band observed at 1433 cm^{-1} is attributed to the C–H bending vibration. The wide band at 1160 and 926 cm^{-1} are the stretching vibrations of the ether bonds of the HEC backbone (asymmetric and symmetric) (Kamarudin and Isa 2013). In addition, the peak at 1372 cm^{-1}, ascribed to C–OH stretching (Li et al. 2015). The spectrum of CX is shown in Fig. 2b. The band at 847 cm^{-1} can be attributed to the P–C stretching vibration, and the absorption band at 706 cm^{-1} characterized to P = S groups of CX (Kassem et al. 2017). The HEC/AAc hydrogel is shown in Fig. 2c; the peak at 1706 cm^{-1} is attributed to the ester bond that formed between acrylic acid and HEC (Chen et al.

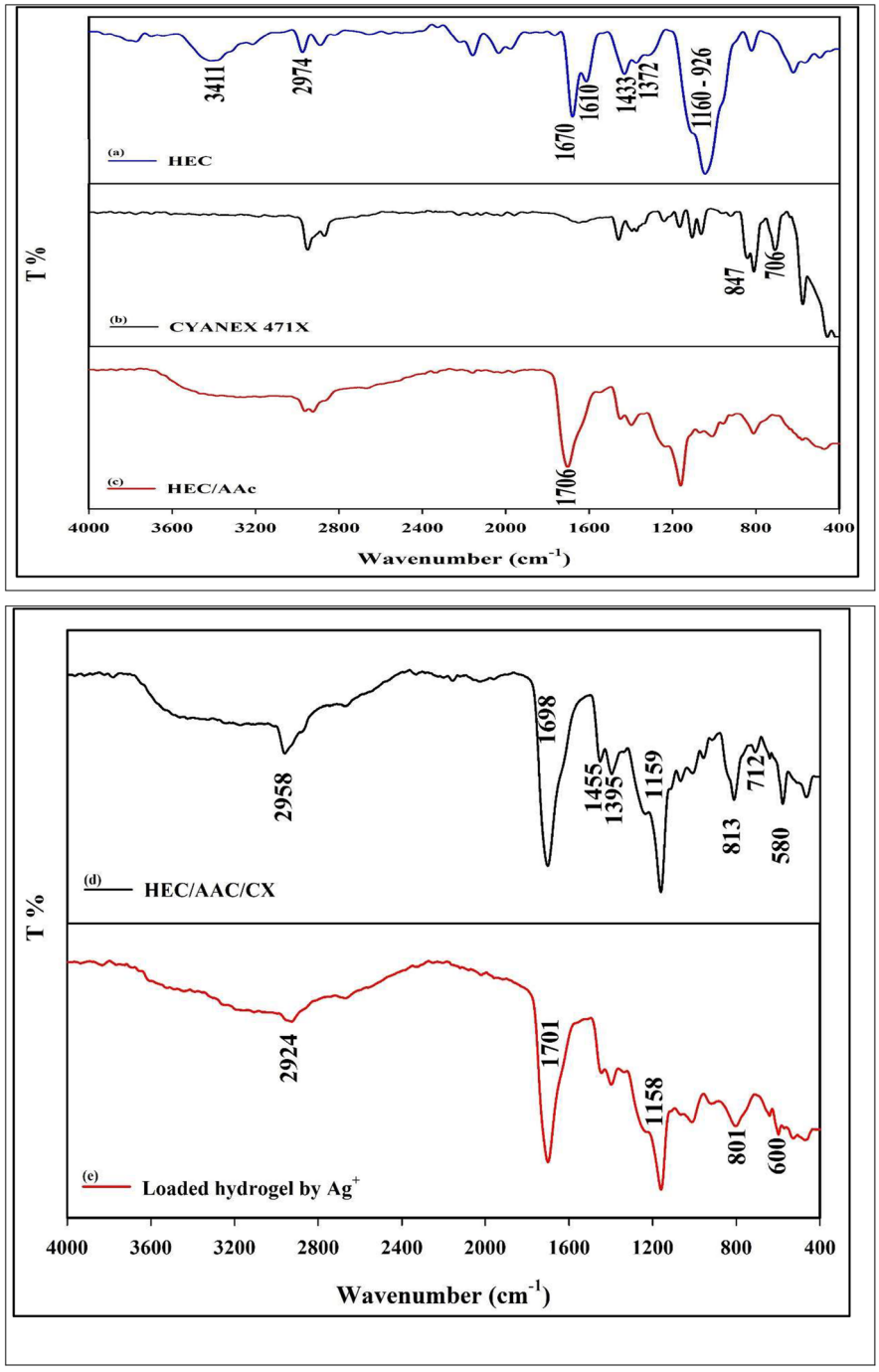

Fig. 2 FTIR spectra of hydroxyethyl cellulose **a**, CX **b**, HEC/AAc **c**, HEC/AAc/ CX **d**, and HEC/AAc/CX hydrogel after Ag uptake **e**

2009). The spectrum of HEC/AAc/ CX hydrogel is shown in Fig. 1d. The new absorption bands at 813 and 712 cm^{-1} are ascribed to P–C and P = S groups in CX, which confirms the formation of HEC/AAc/ CX hydrogel in the presence of CX by radiation technique. After the silver absorption process, the band at 624 cm^{-1} appears in Fig. 1e, and it is believed that it is due to the formation of the S–Ag bond.

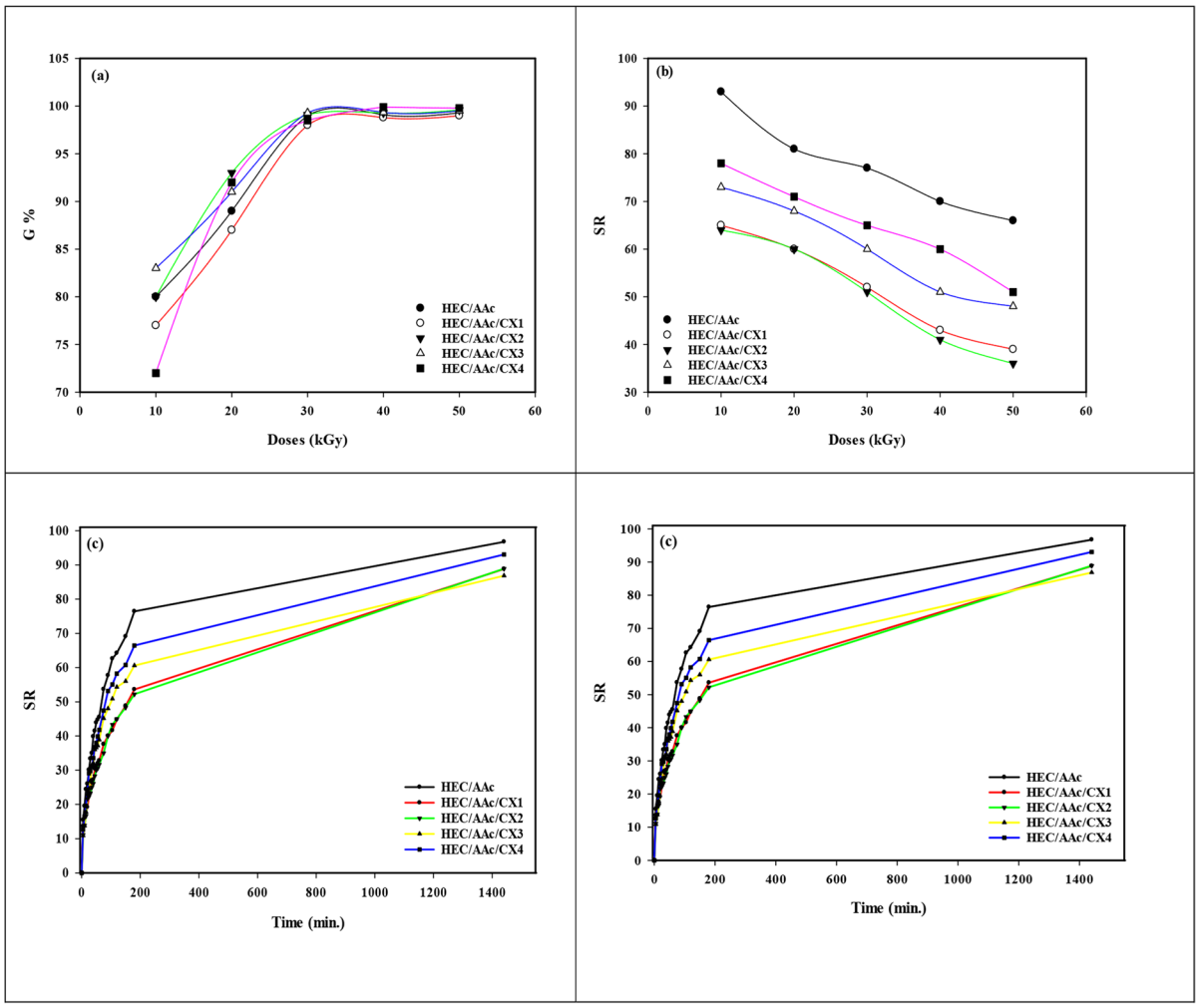

Fig. 3 **a** Gel content of prepared hydrogels (HEC/AAc, HEC/AAc/CX 1, 2, 3 and 4) with different irradiation doses, **b** Hydrogels' swelling ratios at various radiation dosages, **c** Hydrogels' swelling ratios as a function of time at 25 ˚C and **d** swelling kinetics of different hydrogels

The gel content, swelling degree and swelling kinetics of the hydrogels

The gel fraction and water absorption represent crucial characteristics of a hydrogel, particularly in relation to its suitability for applications involving metal adsorption capability. It is clear from Fig. 3a that with increasing irradiation doses, the gel content increases as gamma rays increase the density of the irradiated hydrogels (Dafader et al. 2012). With the increase in density, the gel content increases.

Table 2 Diffusion parameters of the HEC/AAc, HEC/AAc/CX1, HEC/AAc/CX2, HEC/AAc/CX3 and HEC/AAc/CX4

Hydrogels	R^2	N	Mechanism
HEC/AAc	0.995	0.46	Fickian
HEC/AAc/CX1	0.984	0.41	Fickian
HEC/AAc/CX2	0.994	0.44	Fickian
HEC/AAc/CX3	0.986	0.51	non-Fickian
HEC/AAc/CX4	0.993	0.48	Fickian

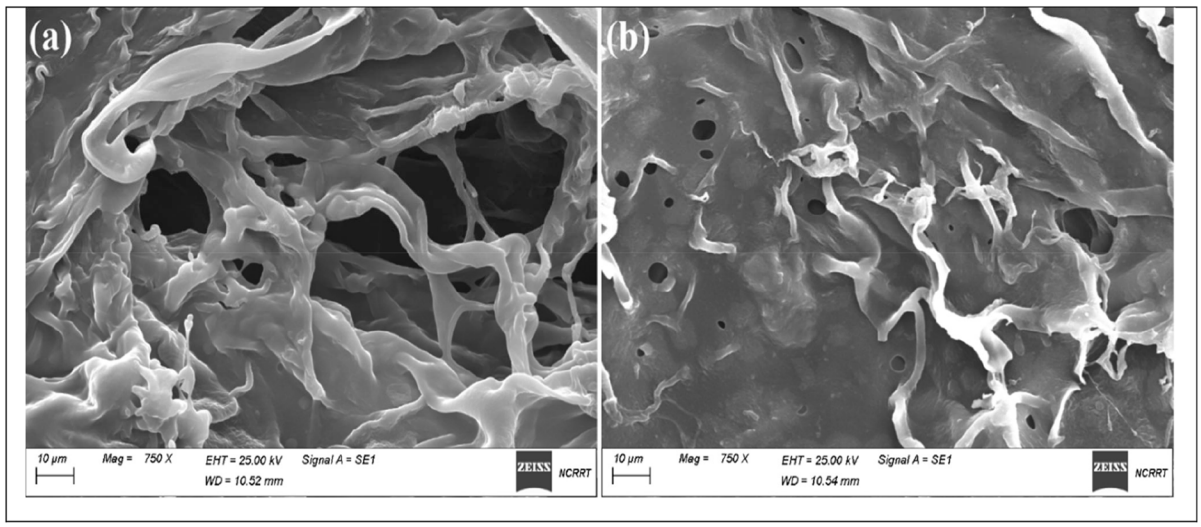

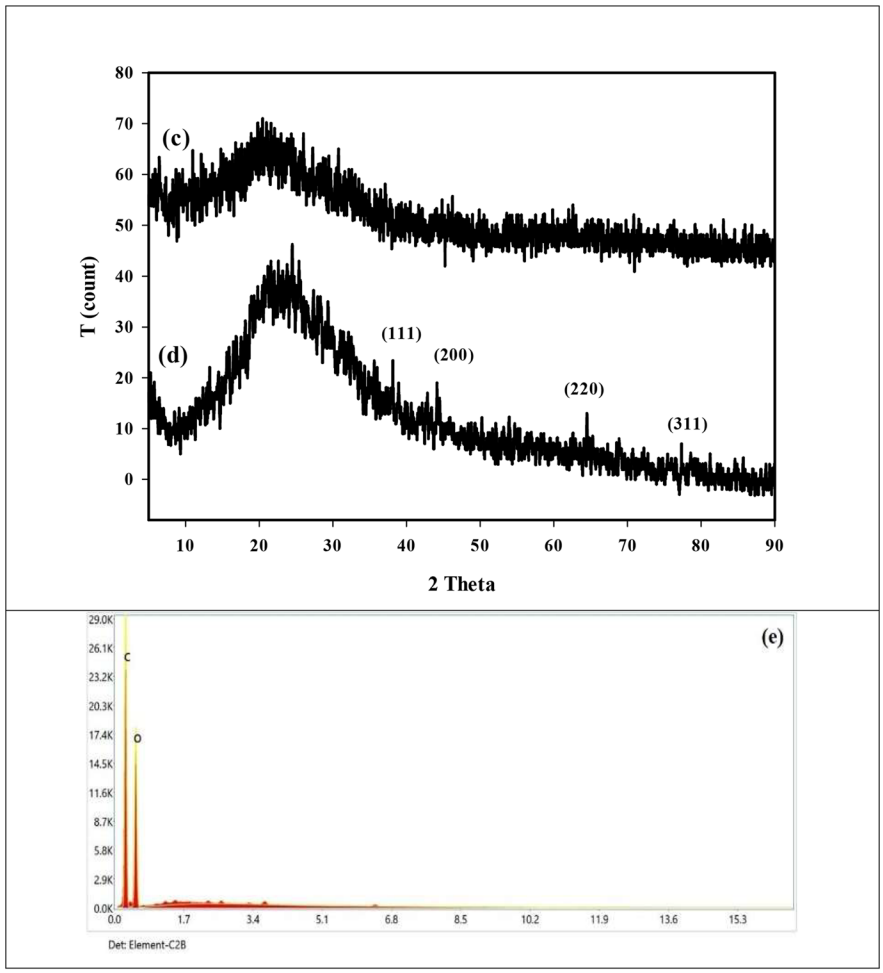

Fig. 4 SEM photographs of hydrogels (**a**) before sorption of Ag ions (magnification × 500) and (**b**) after sorption of Ag ions (magnification × 500), XRD patterns of (**c**) HEC/AAc/CX3 hydrogel and (**d**) Ag-HEC/AAc/CX3 hydrogel, EDX –measurements of (**e**) HEC/AAc, (**f**) HEC/AAc/CX3 and (**g**) HEC/AAc/CX3 (Ag^{+})

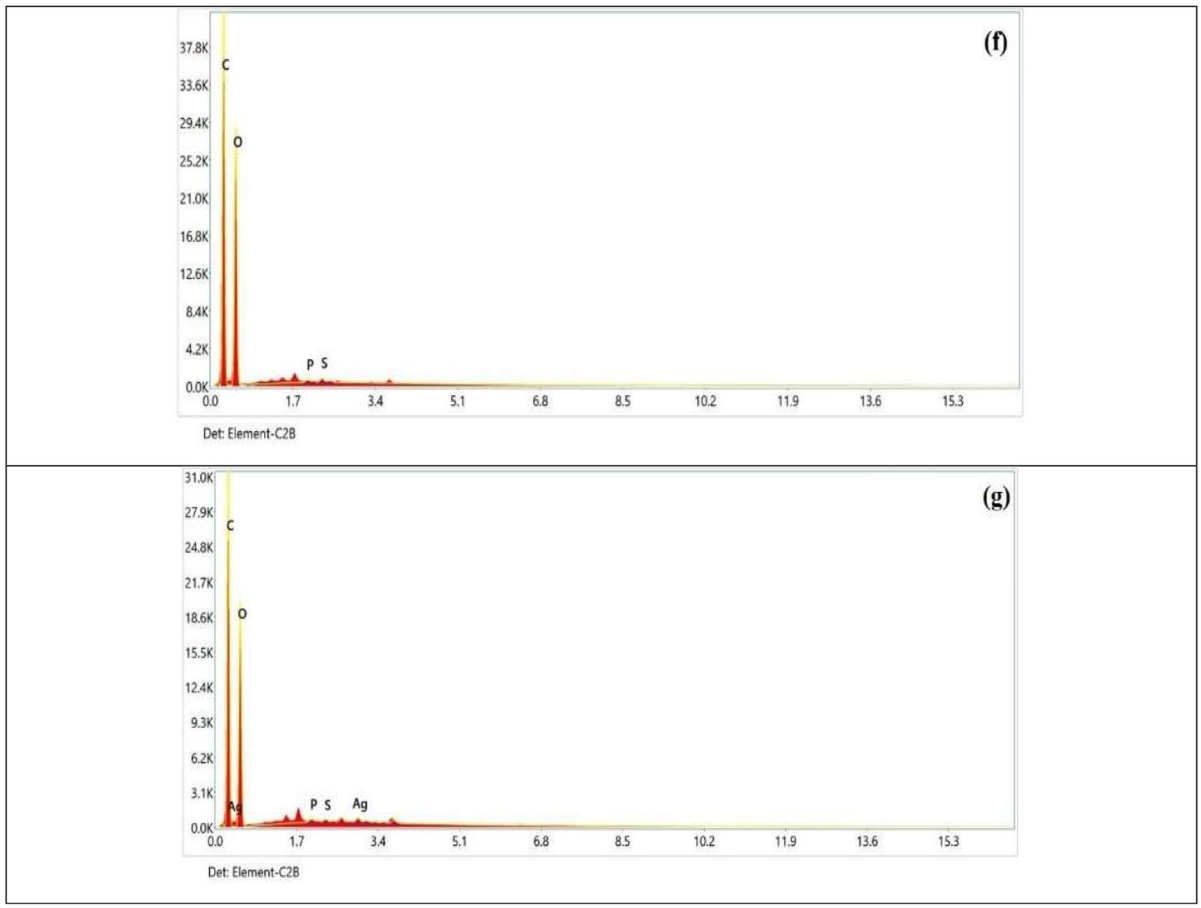

Fig. 4 (continued)

The gel content of HEC/AAc/CX3 increased from 83 to 91% with an increase in radiation dose from 10 to 20 kGy. With a further increase in the radiation dose to 30 kGy, the gel content reached 99.3%, and it remained stable even with an increase in the radiation dose to 50 kGy. At radiation doses less than 30 kGy, the gelation content is unsatisfactory in terms of physical properties to withstand some applications. In the study of the swelling ratio with different irradiation doses, Fig. 3b describes the change in the swelling rate. The swelling rate decreases with increasing radiation doses as a result of increasing the density of the prepared hydrogel network (Mohamad et al. 2017). The swelling ratio of HEC/AAc hydrogel reduced from 93 to 66 as the radiation dose elevated from 10 to 50 kGy. Also, the swelling degree decreased from 65, 64, 73, and 78 to 39, 36, 48, and 51 for HEC/AAc/CX1, HEC/AAc/CX2, HEC/AAc/CX3, and HEC/AAc/CX4, respectively. The swelling ratio is one of the most important parameters necessary for the study of hydrogels, as it is closely related to the application of hydrogels. Figure 3c shows that the swelling ratios of the hydrogels varied with time in distilled water at 25 °C. All the hydrogels reached equilibrium after about three hours. The swelling ratio after 3 h was higher for the HEC/AAc hydrogel (76.4) compared to the different hydrogels, which contain any percentage of CX. The swelling rations were 53.6, 52.2, 60.5, and 66.4 for HEC/AAc/CX1, HEC/AAc/CX2, HEC/AAc/CX3, and HEC/AAc/CX4, respectively. As seen in Fig. 3d and Table 2, the Fickian diffusion model can be successfully applied to the initial swelling process to give straight, fitted linear lines with a good correlation coefficient ($R^2 > 0.98$). The (n) values were in the range of 0.41–0.48 (Fickian diffusion) for HEC/AAc, HEC/AAc/CX1, HEC/AAc/CX2, and HEC/AAc/CX4. But the determined

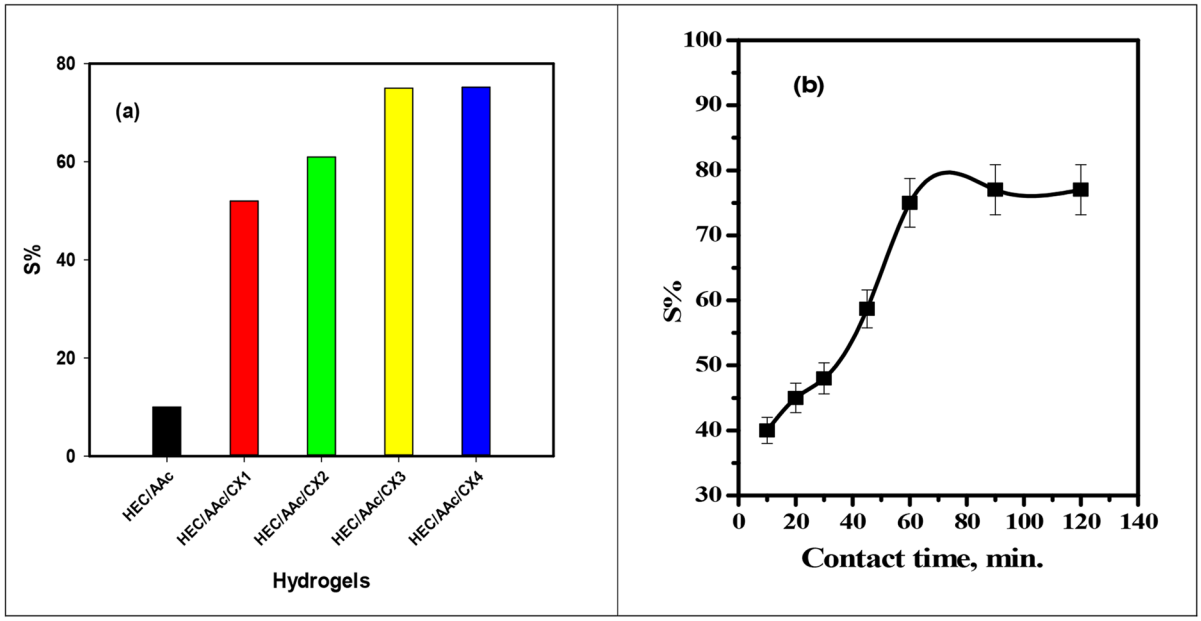

Fig. 5 **a** different hydrogels contains weights of CX for the uptake of Ag ions (**b**) Effect of time on the sorption of Ag(I) using HEC/AAc/CX3 hydrogel from acidic nitrate medium

n was 0.51 for the HEC/AAc/CX3, indicating that the water uptake was controlled collaboratively by water diffusion and relaxation of polymer chains (non-Fickian diffusion); this occurs in those cases where the diffusion and relaxation rates are comparable (Dafader et al. 2011).

SEM, XRD patterns and EDX measurements of HEC/AAc/CX3 hydrogel

The SEM images clearly show that the hydrogels exhibit a porous structure on the inside (Fig. 4a), as well as that the HEC/AAc/CX3 hydrogel, which was prepared by radiation, has large pores as a result of the electrostatic repulsion between the carboxylic anions, which expand the hydrogel network from the inside and outside and are responsible for increasing the size and diameter of the pores. Those pores are responsible for absorbing and assimilating aqueous solutions and minerals (Ma et al. 2008), such as Ag ions. On the other hand, the hydrogel appears after the adsorption process in Fig. 4b, with a different morphology. The pore shapes changed and decreased as a result of reducing the electrostatic repulsion through the adsorption of cationic metal ions (Ag). Also, after the sorption process, hydrogel is more-thick; pores are filled with metal ions after interacting with metal ions. XRD patterns of HEC/AAc/CX3 hydrogels before sorption of silver ions are given in Fig. 4c. and revealed the absence of peaks in pristine hydrogels, which confirmed their non-crystalline nature. Also, in Fig. 4d, Ag/HEC/AAc/CX3 hydrogels after sorption of silver are assigned to diffractions at 2θ values of 38°, 44.2°, 64.41° and 77.43° are assigned to reflections through (111), (200), (220), and (311) planes of the face centered cubic (fcc) of silver nanoparticles, respectively (Thomas et al. 2007). Elemental analysis shows that the HEC/AAc/CX3 hydrogel in the presence of CX contains the elements S and P, and after the absorption process, small percentages of silver appear as a result of the absorption process, as shown in Fig. 4(e–f).

Sorption procedures of Ag(III) onto HEC/AAc/CX3 hydrogels

Preliminary investigations and the effect of equilibrium contact time

The preliminary experimental investigations on the uptake efficiency of the different prepared HEC/AAc/CX hydrogel adsorbents which containing different percentages of CX (Wt %) in the range (0–0.2

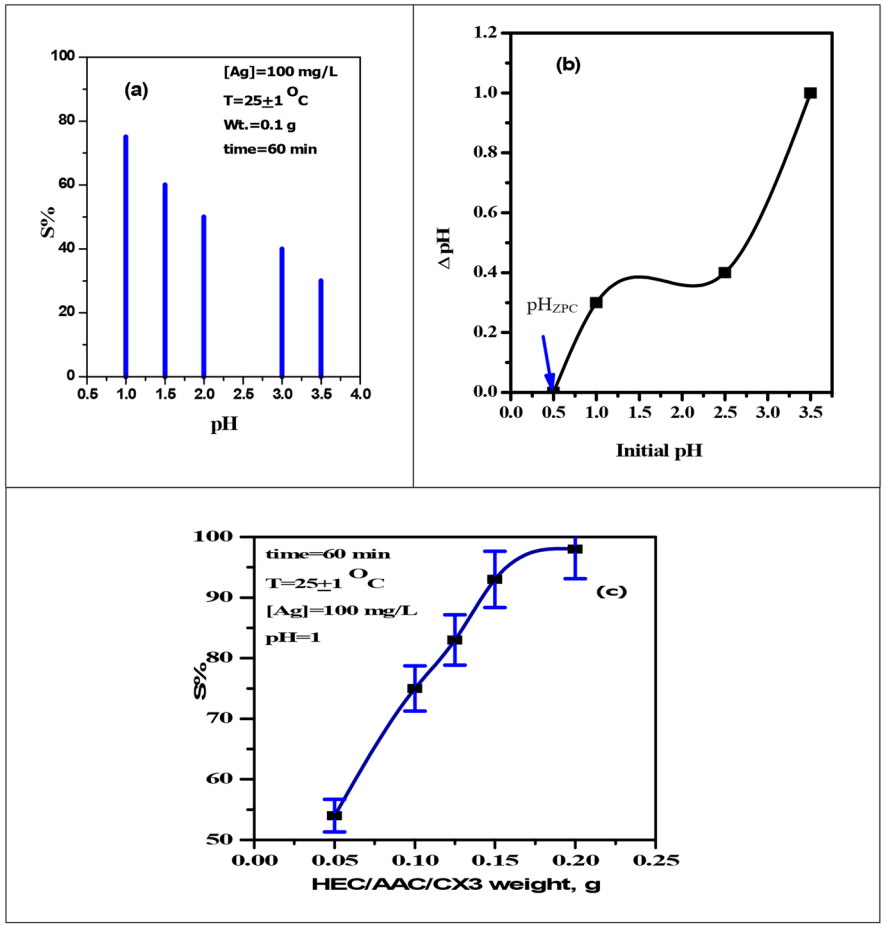

Fig. 6 **a** Effect of solution pH on the sorption of Ag(I) onto HEC/AAc/ CX3 adsorbents, **b** Ph_{Zpc} of HEC/AAc/ CX3 hydrogel, and **c** Effect of HEC/AAc/ CX3 hydrogel weight on the sorption of Ag(I) ions from acidic nitrate medium

g) were carried out. 0.1 g of each adsorbent sample was individually shaking with 5 mL of 100 mg/L Ag(I) at solution pH = 1, time = 60 min. The results plotted in Fig. 5a were indicating that the uptake efficiency takes the order: HEC/AAc/CX4 > HEC/AAc/CX3 > HEC/AAc/CX2 > HEC/AAc/CX1 > HEC/AAc. In this context; irradiate HEC/AAc/CX3 hydrogel was employed for complete batch study for the sorption of Ag(I) from acidic nitrate medium.

The first parameter in this study is the determination of contact equilibrium time for the uptake of 100 mg/L Ag(I) from acidic nitrate medium. This experiment was performed by contact 5 mL of aqueous metal ion solution with 0.1 g of HEC/AAc/CX3 hydrogel in the time range 10 to 120 min and results plotted in Fig. 5b illustrate that the maximum sorption percentage of Ag(I) increased to 75% in the first stage (10–60 min). Further increase in the second stage (60–120 min) show that there was slowly increase in the uptake efficiency of sliver ions and still almost constant; this may be regarding to the saturation of the adsorbent active sites. In concluded the contact equilibrium time was maintained of 60 min all the experiments during these study investigations.

The effect of solution pH

The impact of varied solution pH on the sorption of 100 mg/L of Ag(I) in contact for 60 min with 0.1 g of HEC/AAc/CX3 hydrogel sorbent was carried out in the pH range 1–3.5. According to the data shown in Fig. 6a and the suggested experimental conditions, the sorption efficiency of Ag(I) gradually decreased from 75 to 30% with an increase in pH from 1 to 3.5 M. This extensive decrease could be explained by the significant stepwise desorption rates for adsorbed Ag(I) ions with increasing solution pH. Therefore, the sorption experiments were

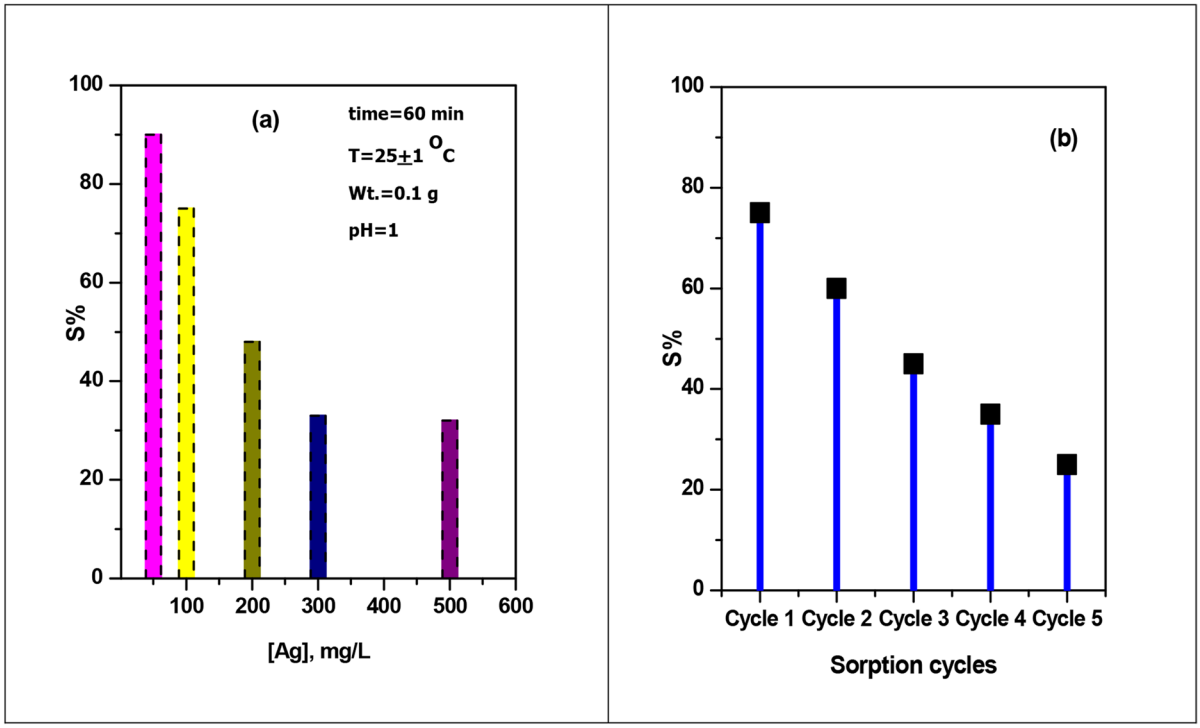

Fig. 7 **a** The initial metal ion concentration on the sorption of Ag ions by HEC/AAc/ CX3 hydrogel from acidic nitrate medium and (**b**) Sorption cycles 100 mg/L of Ag(I) onto HEC/AAc/ CX3 from acidic nitrate medium

conducted at a low pH of 1, which results in an efficiency of 75%. As well as the selection of a low pH of 1, it is important to work in a low-acidic medium so that fission products are dissolved in a highly concentrated acid medium. As a result, the adsorbent's zero-point charge is 0.5, as shown in Fig. 6b, and the adsorbent's surface active sites will be negatively charged when pH exceeds 0.5, making them suitable sites for the cationic species Ag^+ adsorption.

Effect of HEC/AAc/CX hydrogel weight

The effect of HEC/AAc/CX3 hydrogel adsorbent weights in the range of 0.05–0.2 g on the uptake efficiency of 100 mg/L Ag(I) at pH = 1 was investigated. The results represented in Fig. 6c indicated that the uptake percent of Ag(I) ions from an acidic solution at the suggested sorption conditions was increased from 30 to 90% with a gradual increase in weight in the studied range. These results confirmed the high affinity of the composite through increasing adsorption sites and increasing the weight of HEC/AAc/ CX3 hydrogel. Furthermore, 0.1 g was chosen as the optimum ratio in all the experiments, which gave an uptake efficiency of 75% after one sorption cycle under the used experimental conditions.

Effect of the initial Ag(I) concentration

The initial metal ion concentration is an important parameter from which we estimated the sorption isotherm models. From this point, the effect of the initial silver ion concentrations in the range of 50–500 mg/L on its sorption using 0.1 g HEC/AAc/CX3 (5 ml) at solution pH = 1 for 60 min was carried out Fig. 7a. The experimental data show that the uptake percentage decreased with increasing [Ag(I)] and became 35% at 500 mg/L, which indicates that the active sites on the hydrogel adsorbent surface became totally occupied with the formation of stable equilibrium between silver adsorption and desorption cycles.

Sorption capacity

From the batch sorption of Ag(II) using HEC/AAc/ CX3 hydrogels it was clear that the irradiated HEC/

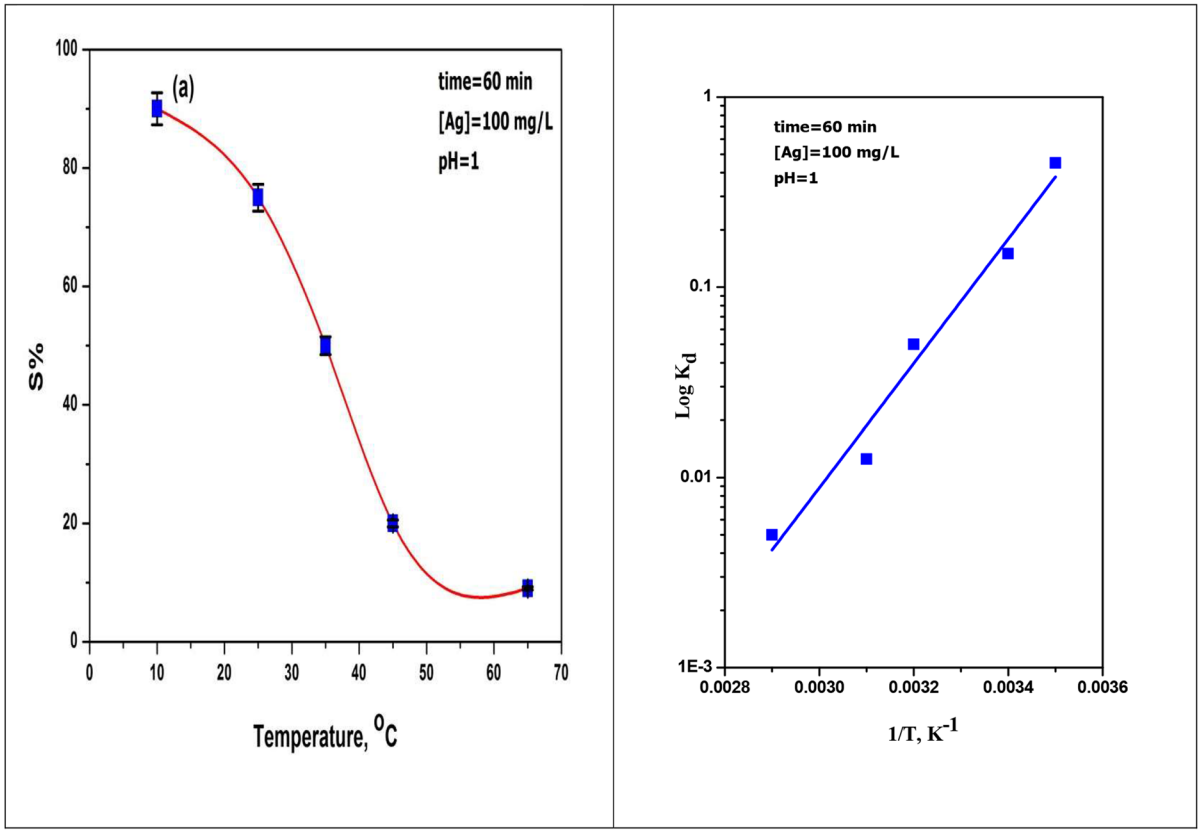

Fig. 8 Plots between: (**a**) the temperature and the sorption % (S %) (**b**) 1/T versus log K_d for S% of Ag(I) ions by HEC/AAc/CX3 hydrogels from nitrate solution

AAc/CX3 hydrogel is more efficient. From this point, the maximum sorption capacity of HEC/AAc/CX3 sorbent with 100 mg/L of Ag(I) under the used experimental conditions (time = 60 min, T = 25 °C, and wt = 0.1 g) was investigated. The sorption step was carried out several times with fresh Ag(I) aqueous solution until low sorption occurred and the maximum capacity ($q_{max}x$) was calculated from Eq. 7 (Çavuş et al. 2006).

$$\text{Max. Capacity}(q_{max}) = \frac{\sum uptake\%}{100} \times C_i \times \frac{V}{m} \qquad (7)$$

Table 3 Thermodynamic parameters for sorption of Ag ions onto HEC/AAc/CX3 hydrogel adsorbent from nitrate medium

Thermodynamic Parameters	ΔH, k J /mol	ΔG, k J /mol	ΔS, J /mol
Value	- 62.60	5	-227

After 5 sorption cycles Fig. 7b, the evaluated q_{max} was found to be 12 mg/g, which confirm the high efficiency of the prepared HEC/AAc/CX3 hydrogels towards the recovery of Ag(I) form acidic solution.

Table 4 Values of desorption efficiency for Ag(I) after sorption on HEC/AAc/CX3 at pH = 1 and 25 ± 1°C

Desorption reagents, M	Conc., M	D%
HNO_3	**1**	**5**
Sulfamic acid	**1**	**42**
HCl	1	7
KSCN	1	27
NH_4SCN	**0.5**	**70**
Thiourea	0.5	35
$NaNO_3$	1	10

Table 5 Comparison of Ag/ HEC/AAc/CX3 system with other reported materials

Adsorbents	Adsorption capacities (mg. g^{-1})	(Ref.)
Chitosan/Montmorillonite Composite	5.0	(Jintakosol and Nitayaphat 2016)
Low-rank Turkish coals	1.87	(Karabakan et al. 2004)
Peat	5.50	(Hanzlik et al. 2004)
Fly ash	6.48	(Çoruh et al. 2011)
CTS/BC	52	(Nitayaphat and Jintakosol 2015)
Expanded perlite	8.60	(Ghassabzadeh et al. 2010)
HEC/AAc/CX3	12	Current work

Thermodynamic parameters calculations for HEC/ AAc/ CX3

The effect of temperature on the sorption of 100 mg/L Ag ions from acidic nitrate medium using HEC/AAc/CX3 hydrogel was studied in the range (10–65 °C) at the selected experimental conditions (contact time = 60 min, pH = 1and V/m = 0.05 L/g). The results plotted in Fig. 8a; show that the sorption efficiency was decreased with increasing temperature and this could be attributed to an increase in the elasticity of the prepared HEC/AAc/ CX3, which make changes in the adsorbent active sites. The values of thermodynamic parameters such as enthalpy (ΔH) and entropy (ΔS) changes were obtained from the linear plot of 1/T vis log K_d, Fig. 8b; and were calculated from Eq. (8–9) (Elkony et al. 2023; Ibrahim et al. 2020).

$$\log K_d = \frac{\Delta S}{2.303R} - \frac{\Delta H}{2.303RT} \tag{8}$$

$$\Delta G = \Delta H - T\Delta S \tag{9}$$

where T is the temperature in Kelvin (K), R is the gas constant (8.314 J $mol^{-1}K^{-1}$) and K_d is the distribution coefficient (mL/g). The values of thermodynamic parameters reported are given in Table 3; the negative ΔH indicates the exothermic nature of the silver sorption process on HEC/AAc/CX3, the negative value of ΔS indicates the decrease of disordering of the reaction system and the positive value of ΔG indicates that the reaction is a nonspontaneous process.

Desorption and regeneration HEC/AAc/CX

Utilizing several stripping agents, including HNO_3, sulfamic acid, HCl, KSCN, NH_4SCN, $NaNO_3$, and thiourea for desorption of Ag ions sorbed by HEC/ AAc/CX3. The experiment's findings given in Table 4 demonstrated that the desorption percentage (D%) of Ag ions using NH_4SCN (0.5 M) was accomplished entirely after two cycles (first = 70% and second = 30%) under the desorption step's applied experimental circumstances (Time = 60 min, V/m = 0.05 L/g, T = 25 °C). The regenerated HEC/AAc/CX3 was employed for others sorption cycles for silver ions under the experimental conditions used.

Comparison of Ag/ HEC/AAc/CX3 system with other reported materials

To take advantage of the HEC/AAc/CX3 hydrogel for Ag uptake from an aqueous acidic solution, a comparative study was investigated with adsorption capacities reported for several adsorbents for Ag recovery from aqueous solutions (3, 17, 21, 24, 36) in Table 5. The HEC/AAc/CX3 hydrogel was discovered to have a moderate adsorption capacity compared to certain other adsorbents. This finding suggests that HEC/ AAc/CX3 beads can be used as effective adsorbents for Ag and $^+$ retention in an aqueous acidic solution.

Conclusions

* HEC/AAc/CX3 hydrogel was prepared via gamma radiation at 30 kGy and was characterized using different characterization, including FT-IR, SEM, XRD, and EDX.

* The Fickian diffusion model results indicate that HEC/AAc/CX3 hydrogel is non-Fickian diffusion.
* Under the utilized experimental circumstances (time = 60 min, [Ag] = 100 mg/L, T = 25 °C, V/m = 0.05 L/g, and pH = 1), the sorption efficiency was found to be 75%.
* HEC/AAc/CX3 adsorbent's zero-point charge was found to be 0.5 through the results of the measured solution pH.
* The maximum sorption capacity of HEC/AAc/CX3 was found to be 12 mg/g at V/m = 0.05 L/g.
* The sorption process is exothermic and nonspontaneous, according to the calculated thermodynamic parameters.
* The maximum desorption efficiency of 70% was achieved using 0.5 M NH_4SCN after one desorption cycle.
* The regenerate HEC/AAc/CX3 can be used for other different sorption cycles.
* HEC/AAc/CX3 hydrogel adsorbent has a good, appropriate capacity compared with other adsorbents.

Acknowledgments Authors are thankful to the Egyptian Atomic Energy Authority for its continuous support for scientific research and development.

Author contribution Botros A. Masry: conceptualization, investigation, methodology, writing original draft, writing review and editing. Hany M. Gayed: Methodology, formal analysis, investigation, writing original draft, review and editing.Jacqueline A. Daoud: supervision, conceptualization, methodology, writing original draft, writing review and editing.

Funding Open access funding provided by The Science, Technology & Innovation Funding Authority (STDF) in cooperation with The Egyptian Knowledge Bank (EKB).

Data availability No data was used for the research described in the article. The data presented in this study are available in the article.

Declarations

Ethics approval Not applicable.

Contest to participate Not applicable.

Contest for publication Not applicable.

Competing interests The authors declare no competing interests.

References

Abd El-Ghaffar M, Mohamed M, Elwakeel KZ (2009) Adsorption of silver (I) on synthetic chelating polymer derived from 3-amino-1, 2, 4-triazole-5-thiol and glutaraldehyde. Chem Eng J 151:30–38

Ahmed I, Nayl A, Daoud J (2011) Extraction of palladium from nitrate solution by CYANEX 471X. Int J Miner Process 101:89–93

Allahyar N, Özeroğlu C (2022) Kinetics and equilibrium study of the adsorption of silver ions by polymeric composites containing zeolite and methacrylic acid. J Iran Chem Soc 1–12

Aly M, Masry B, Daoud J (2021) Liquid-liquid extraction of platinum (IV) from acidic nitrate medium using a commercial trialkyl phosphine oxide in kerosene. Sep Sci Technol 56:2596–2608

Aly M, Hassan M, Ghobashy M, Masry B (2022) Removal of barium (II), cobalt (II), and strontium (II) from aqueous solution using chemically modified poly (acrylonitrile-butadiene-styrene) pellets. Part Sci Technol 40:697–711

Ashfaq A, Clochard M-C, Coqueret X, Dispenza C, Driscoll MS, Ulański P, Al-Sheikhly M (2020) Polymerization reactions and modifications of polymers by ionizing radiation. Polymers (Basel) 12:2877

Bajpai SK, Dubey S (2004) Synthesis and swelling kinetics of a pH-sensitive terpolymeric hydrogel system. Iran Polym J 13:189–203

Behera S, Mahanwar PA (2020) Superabsorbent polymers in agriculture and other applications: a review. Polym-Plast Technol Mater 59:341–356

Bundjaja V, Santoso SP, Angkawijaya AE, Yuliana M, Soetaredjo FE, Ismadji S, Ayucitra A, Gunarto C, Ju Y-H, Ho M-H (2021) Fabrication of cellulose carbamate hydrogel-dressing with rarasaponin surfactant for enhancing adsorption of silver nanoparticles and antibacterial activity. Mater Sci Eng C 118:111542

Çavuş S, Gürdağ G, Yaşar M, Güçlü K, Gürkaynak, MA (2006) The competitive heavy metal removal by hydroxyethyl cellulose-g-poly (acrylic acid) copolymer and its sodium

salt: the effect of copper content on the adsorption capacity. Polym Bull 57:445–456
Çelik Z, Gülfen M, Aydın AO (2010) Synthesis of a novel dithiooxamide–formaldehyde resin and its application to the adsorption and separation of silver ions. J Hazard Mater 174:556–562
Chen R, Yi C, Wu H, Guo S (2009) Solid state mechano-chemical grafting copolymerization of hydroxyethyl cellulose with acrylic acid. J Appl Polym Sci 112:3537–3542
Çoruh S, Elevli S, Şenel G, Ergun ON (2011) Adsorption of silver from aqueous solution onto fly ash and phosphogypsum using full factorial design. Environ Prog Sustain Energy 30:609–619
Dafader N, Adnan M, Haque M, Huq D, Akhtar F (2011) Study on the properties of copolymer hydrogel obtained from acrylamide/2-hydroxyethyl methacrylate by the application of gamma radiation. Afr J Pure Appl Chem 5:111–118
Dafader N, Akter T, Haque M, Swapna S, Islam S, Huq D (2012) Effect of acrylic acid on the properties of polyvinylpyrrolidone hydrogel prepared by the application of gamma radiation. Afr J Biotechnol 11:13049–13057
Duche S, Chavan D, Dhadke P (2002) Extraction Behaviour of Cyanex-923 and Cyanex-471X Towards the Rhodium (III) from Bromide Media and Its Separation from other Platinum Metals. J Chin Chem Soc 49:165–172
Elella MHA, Goda ES, Gab-Allah MA, Hong SE, Pandit B, Lee S, Gamal H, Ur Rehman A, Yoon KR (2021) Xanthan gum-derived materials for applications in environment and eco-friendly materials: A review. J Environ Chem Eng 9:104702
Elkony AM, Ibrahim AG, Abu El-Farh MH, Abdelhai F (2023) Synthesis of Acrylamide-co-3-Allyloxy-2-hydroxy-1-propanesulfonic acid sodium salt Hydrogel for efficient Adsorption of Methylene blue dye. Int J Environ Anal Chem 103:1751–1770
Fleitlikh IY, Grigorieva N, Pavlenko N, Kondrasenko A, Tikhonov AY, Logutenko O (2019) Synergistic silver extraction from hydrochloric acid solutions with triisobutylphosphine sulfide in the presence of organic proton-donor additives. Solv Extrac Ion Exch 37:96–109
Foroughi F, RezvaniGhomi E, MorshediDehaghi F, Borayek R, Ramakrishna S (2021) A review on the life cycle assessment of cellulose: From properties to the potential of making it a low carbon material. Materials (Basel) 14:714
Gayeda HM, Abou El Fadla FI, Maziada NA, El-Aassarb AHM, Abdel-Mottalebc M (2019) Surface modification of composite polyamide reverse osmosis membrane by irradiated chitosan and TiO. Water Treat 1:9
Ghassabzadeh H, Mohadespour A, Torab-Mostaedi M, Zaheri P, Maragheh MG, Taheri H (2010) Adsorption of Ag, Cu and Hg from aqueous solutions using expanded perlite. J Hazard Mater 177:950–955
Gulrez SK, Al-Assaf S, Phillips G (2011) Hydrogels: methods of preparation, characterisation and applications. Prog mol environ bioengin analysis mode techn applic 117150
Gupta B, Singh I, Mahandra H (2014) Extraction and separation studies on Pt (IV), Ir (III) and Rh (III) using sulphur containing extractant. Sep Purif Technol 132:102–109
Hanzlik P, Jehlicka J, Weishauptova Z, Sebek O (2004) Adsorption of copper, cadmium and silver from aqueous solutions onto natural carbonaceous materials. Plant Soil Environ 50:257–264
Hou H, Yu D, Hu G (2015) Preparation and properties of ion-imprinted hollow particles for the selective adsorption of silver ions. Langmuir 31:1376–1384
Huang Y, Zhao W, Zhang X, Peng H, Gong Y (2019) Thiolene synthesis of thioether/carboxyl-functionalized polymers for selective adsorption of silver (I) ions. Chem Eng J 375:121935
Ibrahim AG, Sayed AZ, Abd El-Wahab H, Sayah MM (2020) Synthesis of a hydrogel by grafting of acrylamide-co-sodium methacrylate onto chitosan for effective adsorption of Fuchsin basic dye. Int J Biol Macromol 159:422–432
Jacob S, Nair AB, Shah J, Sreeharsha N, Gupta S, Shinu P (2021) Emerging role of hydrogels in drug delivery systems, tissue engineering and wound management. Pharmaceutics 13:357
Janmohammadi M, Nazemi Z, Salehi AOM, Seyfoori A, John JV, Nourbakhsh MS, Akbari M (2023) Cellulose-based composite scaffolds for bone tissue engineering and localized drug delivery. Bioact Mater 20:137–163
Jin W, Zhang Y (2020) Sustainable electrochemical extraction of metal resources from waste streams: from removal to recovery. ACS Sustain Chem Eng 8:4693–4707
Jintakosol T, Nitayaphat W (2016) Adsorption of silver (I) from aqueous solution using chitosan/montmorillonite composite beads. Mater Res 19:1114–1121
Kabir SF, Sikdar PP, Haque B, Bhuiyan MR, Ali A, Islam M (2018) Cellulose-based hydrogel materials: Chemistry, properties and their prospective applications. Prog Biomater 7:153–174
Kajjari PB, Manjeshwar LS, Aminabhavi TM (2011) Semi-interpenetrating polymer network hydrogel blend microspheres of gelatin and hydroxyethyl cellulose for controlled release of theophylline. Ind Eng Chem Res 50:7833–7840
Kamarudin K, Isa M (2013) Structural and DC Ionic conductivity studies of carboxy methylcellulose doped with ammonium nitrate as solid polymer electrolytes. Int J Phys Sci 8:1581–1587
Kang H, Liu R, Huang Y (2015) Graft modification of cellulose: Methods, properties and applications. Polymer 70:A1–A16
Karabakan A, Karabulut S, Denizli A, Yürüm Y (2004) Removal of silver (I) from aqueous solutions with low-rank Turkish coals. Adsorpt Sci Technol 22:135–144
Kassem A, Masry B, Zeid M, Noweir H, Saad E, Daoud J (2017) Extraction of palladium from nitrate medium by emulsion liquid membrane containing CYANEX 471X as carrier Solvent. Extr Ion Exch 35:145–160
Krklješ A, Nedeljković J, Kačarević-Popović Z (2007) Fabrication of Ag-PVA hydrogel nanocomposite by γ-irradiation. Polym Bull 58:271–279
Kumar H, Christopher L (2017) Recent trends and developments in dissolving pulp production and application. Cellul 24:2347–2365
Li Q, Gong J, Zhang J (2015) Rheological properties and microstructures of hydroxyethyl cellulose/poly (acrylic acid) blend hydrogels. J Macromol Sci B 54:1132–1143

Li X, Wang Y, Cui X, Lou Z, Shan W, Xiong Y, Fan Y (2018) Recovery of silver from nickel electrolyte using corn stalk-based sulfur-bearing adsorbent. Hydrometallurgy 176:192–200

Liu X, Yang L, Luo X, Pei J, Xi Y, Liu C, Liu L (2018) A novel non-imprinted adsorbent with superior selectivity towards high-performance capture of Ag (I). Chem Eng J 348:224–231

Ma J, Zhang L, Fan B, Xu Y, Liang B (2008) A novel sodium carboxymethylcellulose/poly (N-isopropylacrylamide)/ Clay semi-IPN nanocomposite hydrogel with improved response rate and mechanical properties. J Polym Sci B Polym Phys 46:1546–1555

Madduma-Bandarage US, Madihally SV (2021) Synthetic hydrogels: Synthesis, novel trends, and applications. J Appl Polym Sci 138:50376

Masry BA, Daoud JA (2021) Sorption behavior of tungsten and molybdenum on TVEX-TOPO resin from nitric acid solution. J Chem Technol Biotechnol 96:1399–1410

Masry BA, Zeid MM, Kassem AT, Noweir HG, Saad EA, Daoud JAM (2018) Liquid-liquid extraction and recovery of Pd (II) from nitric acid medium using green diesel as extractant. J Phys Sci 29:25–48

Masry BA, Madbouly H, Daoud JA (2023a) Studies on the potential use of activated carbon from guava seeds (AC-GS) as a prospective sorbent for the removal of Cr (VI) from aqueous acidic medium. Int J Environ Anal Chem 103:378–395

Masry BA, Elhady MA, Mousaa IMJI, Chemistry N-M (2023b) Fabrication of a novel polyvinylpyrrolidone/abietic acid hydrogel by gamma irradiation for the recovery of Zn Co, Mn and Ni from aqueous acidic solution. Inorg Nano-Metal Chem 53:283–294

Maziad NA, Abou El Fadl FI, El-Kelesh NA, El-Hamouly SH, Zeid IF, Gayed HM (2016) Radiation synthesis and characterization of super absorbent hydrogels for controlled release of some agrochemicals. J Radioanal Nucl Chem 307:513–521

Min X, Wu X, Shao P, Ren Z, Ding L, Luo X (2019) Ultrahigh capacity of lanthanum-doped UiO-66 for phosphate capture: Unusual doping of lanthanum by the reduction of coordination number. Chem Eng J 358:321–330

Mingcheng Y, Hongyan S, Chengshen Z, Suqin H (2007) Radiation synthesis and characterization of polyacrylic acid hydrogels. Nucl Sci Tech 18:82–85

Mohamad N, Buang F, Mat Lazim A, Ahmad N, Martin C, Mohd Amin MCI (2017) Characterization and biocompatibility evaluation of bacterial cellulose-based wound dressing hydrogel: effect of electron beam irradiation doses and concentration of acrylic acid. J Biomed Mater Res 105:2553–2564

Mohapatra S, Mirza MA, Hilles AR, Zakir F, Gomes AC, Ansari MJ, Iqbal Z, Mahmood S (2021) Biomedical application, patent repository, clinical trial and regulatory updates on hydrogel: An extensive review. Gels 7:207

Nitayaphat W, Jintakosol T (2015) Removal of silver (I) from aqueous solutions by chitosan/bamboo charcoal composite beads. J Clean Prod 87:850–855

Noweir H, Masry B, Zeid M, Kassem A, Daoud J (2021) Sorption of Mo (VI) from nitric acid solution using SM-4 copolymer resin impregnated with CYANEX 923. J Inorg Organomet Polym 31:1576–1589

Oprea M, Voicu S (2020) Recent advances in composites based on cellulose derivatives for biomedical applications. Carbohydr Polym 247:116683

Padil VV, Wacławek S, Černík M, Varma RS (2018) Tree gum-based renewable materials: Sustainable applications in nanotechnology, biomedical and environmental fields. Biotechnol Adv 36:1984–2016

Qi X, Tong X, Pan W, Zeng Q, You S, Shen J (2021) Recent advances in polysaccharide-based adsorbents for wastewater treatment. J Clean Prod 315:128221

Raafat AI, Eid M, El-Arnaouty MB (2012) Radiation synthesis of superabsorbent CMC based hydrogels for agriculture applications. Nucl Instrum Methods Phys Res, Sect.B 283:71–76

Rimdusit S, Somsaeng K, Kewsuwan P, Jubsilp C, Tiptipakorn S (2012) Comparison of gamma radiation crosslinking and chemical crosslinking on properties of methylcellulose hydrogel. Eng J 16:15–28

Sabbagh F, Muhamad II, Pa'e N, Hashim Z (2019) Strategies in improving properties of cellulose-based hydrogels for smart applications. Cellul-based super hydr 887–908

Saini KJP (2017) Preparation method, properties and crosslinking of hydrogel: a review. PharmaTutor 5:27–36

Sannino A, Demitri C, Madaghiele M (2009) Biodegradable cellulose-based hydrogels: design and applications. Materials (Basel) 2:353–373

Saraydın D, Işıkver Y, Karadağ E (2018) A Study on the correlation between adsorption and swelling for poly (Hydroxamic Acid) hydrogels-triarylmethane dyes systems. J Polym Environ 26:3924–3936

Shao P, Tian J, Duan X, Yang Y, Shi W, Luo X, Cui F, Luo S, Wang S (2019) Cobalt silicate hydroxide nanosheets in hierarchical hollow architecture with maximized cobalt active site for catalytic oxidation. Chem Eng J 359:79–87

Song X, Li C, Xu R, Wang K (2012) Molecular-ion-imprinted chitosan hydrogels for the selective adsorption of silver (I) in aqueous solution. Ind Eng Chem Res 51:11261–11265

Sun M-T, Song F-P, Zhang G-D, Li J-Z, Wang F (2021) Polymeric superabsorbent hydrogel-based kinetic promotion for gas hydrate formation. Fuel 288:119676

Süren SM, Tutar R, Özeroğlu C, Karakuş S (2023) Versatile multi-network hydrogel of acrylamide, sodium vinyl sulfonate, and n, n′-methylene bisacrylamide: a sustainable solution for paracetamol removal and swelling behavior. J Polym Environ 1–18

Thomas V, Yallapu MM, Sreedhar B, Bajpai S (2007) A versatile strategy to fabricate hydrogel–silver nanocomposites and investigation of their antimicrobial activity. J Colloid Interf Sci 315:389–395

Tran TH, Okabe H, Hidaka Y, Hara K (2019) Equilibrium and kinetic studies for silver removal from aqueous solution by hybrid hydrogels. J Hazard Mater 365:237–244

Yu H, Shao P, Fang L, Pei J, Ding L, Pavlostathis SG, Luo X (2019) Palladium ion-imprinted polymers with PHEMA polymer brushes: role of grafting polymerization degree in anti-interference. Chem Eng J 359:176–185

Zou L, Shao P, Zhang K, Yang L, You D, Shi H, Pavlostathis SG, Lai W, Liang D, Luo X (2019) Tannic acid-based adsorbent with superior selectivity for lead (II) capture: Adsorption site and selective mechanism. Chem Eng J 364:160–166

Zulkifli FH, Hussain FSJ, Zeyohannes SS, Rasad MSBA, Yusuff MM (2017) A facile synthesis method of hydroxyethyl cellulose-silver nanoparticle scaffolds for skin tissue engineering applications. Mater Sci Eng C Mater Biol Appl 79:151–160